

# Åland churches as archives of tree-ring records sensitive to fluctuating climate

SAMULI HELAMA<sup>1\*</sup> and THOMAS S. BARTHOLIN<sup>2</sup>

<sup>1</sup>Natural Resources Institute Finland, Eteläranta 55, P.O. Box 16, FI 96301 Rovaniemi, Finland;  
 e-mail: samuli.helama@luke.fi

<sup>2</sup>Scandinavian Dendro Dating, Am Haidberg 18, D 21 465 Wentorf bei Hamburg, Germany;  
 e-mail: thomas.bartholin@gmx.de

Received 24 August 2018; accepted for publication 30 January 2019

**ABSTRACT.** Tree-ring chronologies provide high-resolution late Quaternary palaeoclimatic data. An important aim of tree-ring research is to extend the chronologies back in time, before the period covered by old living trees. Tree-ring material from historic buildings offers an opportunity to develop long chronologies that, in some regions, may cover the period of the past millennium. Such materials have remained in conditions favourable to preservation and can be used to date the construction timber by means of dendrochronology. Apart from dating, tree-ring data may prove valuable in interpreting past climatic conditions. Here we analyse the data of 111 Scots pine (*Pinus sylvestris* L.) tree-ring series from the Åland Islands in south-western Finland. In so doing, we illustrate the variation of wetness and drought in the region over a historical time frame (1057–1826). Non-climatic trends were removed from these series using alternative types of detrending procedures. Tree-ring chronologies constructed from the same raw data but using different types of detrending methods agreed on annual to sub-centennial scales. The chronologies produced using regional curve standardization (RCS), preferably combined with implementation of a signal-free approach, were comparable with previously published sedimentary and tree-ring evidence from the same region. While non-RCS methods are effective in removing non-climatic information from the chronology, they also resulted in removal of the long-term variation (low-frequency), which did, at least in our data, represent the palaeoclimatic signal common to different types of proxy records. These records, including our data and those of gridded reconstructions developed previously as the *Old World Drought Atlas*, agreed in indicating dry conditions over the pre-1250 period and around the mid-15<sup>th</sup> century. The Åland chronology is characterized by notable fluctuations in the availability of tree-ring samples; the periods with low sample replication probably pinpoint years when large construction projects were suspended on these islands.

**KEYWORDS:** *Pinus sylvestris*, tree-ring, tree growth, dendrochronology, palaeoclimatology

## INTRODUCTION

Dendrochronological records produced from subfossil trunks, archaeological wood and historical timber extend tree-ring chronologies back in time, and provide perspectives on past climate variability prior to the era of instrumental observations. Regional and site chronologies from tree-ring material sampled from historical buildings have recently contributed to the development of late Holocene climate records in Northern Europe (Koprowski et al. 2012, Cooper et al. 2013, Wilson et al. 2013,

Helama et al. 2017a, 2018, Seftigen et al. 2017, Balanzategui et al. 2018). These records benefit from cross-dating, a dendrochronological procedure that makes it possible to align the analysed rings according to an exact calendar-year timeline, and to directly compare the chronologies with other records of climate variability (Fritts 1976, Walker 2005, Hughes 2011). Tree-ring data can provide high-resolution, continuous indications of climate variability on annual to millennial scales.

Another procedure essential to analyses of long tree-ring chronologies is the removal

\* Corresponding author

of non-climatic variation, in particular that related to tree age and competition between trees rather than temperature, moisture and light conditions (Fritts 1976). Such components of unwanted growth variability (i.e. noise) are commonly identified and removed from data using the various methods of tree-ring standardization. However, not all of these methods retain the long-term variation present in the raw data; they may actually modify the low-frequency portion of tree-ring variability (Cook et al. 1995). Such loss of information may lessen the value of the resulting data and even lead to distorted inferences of past climatic phases, events and their magnitudes, at least if not rigorously addressed through the development of chronologies and when interpreting their potential signals of climate. A particular method of tree-ring standardization allowing long-term changes in regional and site chronologies to be preserved is regional curve standardization (RCS), the benefits of which have been increasingly shown to outweigh other methods in this respect (Briffa et al. 1992, 1996, Briffa & Melvin 2011, Helama et al. 2017c).

A long Northern European tree-ring chronology, one that has remained largely unexplored, originates from the Åland Islands, an archipelago in the northern Baltic Sea between the mainlands of Finland and Sweden. This chronology is constructed from Scots pine tree-ring material that was sampled from timbers of historic stone churches on these islands in the course of the 1990s campaign to date their construction (Ringbom et al. 1996, see also Ringbom 2011). This project resulted in a substantial number of tree-ring samples being successfully cross-dated and the chronology for the Åland Islands being established. That work antedates the development of RCS methods; to our knowledge, no analyses of the low-frequency climate signal from these tree-ring data have been carried out. Läänelaid et al. (2012) used the Åland data to correlate the Scots pine tree-ring chronologies constructed around the Baltic Sea in Estonia, Finland, Sweden, Lithuania, Poland and north-western Russia, and compared these results with observed and reconstructed modes of North Atlantic climate variability.

The present study focused on different aspects of the Åland dataset, with special reference to detection of the low-frequency component of its tree-ring variability. State-of-the-art

RCS-type methods were applied to disentangle tree growth variation of biological and climatic origin in the data. We compared the resulting RCS chronology with recently published multi-proxy datasets (Cook et al. 2015, Linderholm et al. 2018) from areas adjacent to the Åland Islands. In this way we demonstrated the potential value of the Åland chronology to the ongoing development of hydroclimatic proxy records in this part of Europe (Sohar et al. 2014, Seftigen et al. 2017, Helama et al. 2017b, 2018, Luoto & Nevalainen 2018) and to the continuing discussion of the late Holocene climate transitions.

## MATERIAL AND METHODS

### STUDY SITES AND MATERIALS

Our study sites include the Åland Islands in south-western Finland (Fig. 1), where previous investigations have identified a substantial amount of material suitable for tree-ring analyses as part of the campaign to study and date the stone churches and their architectural

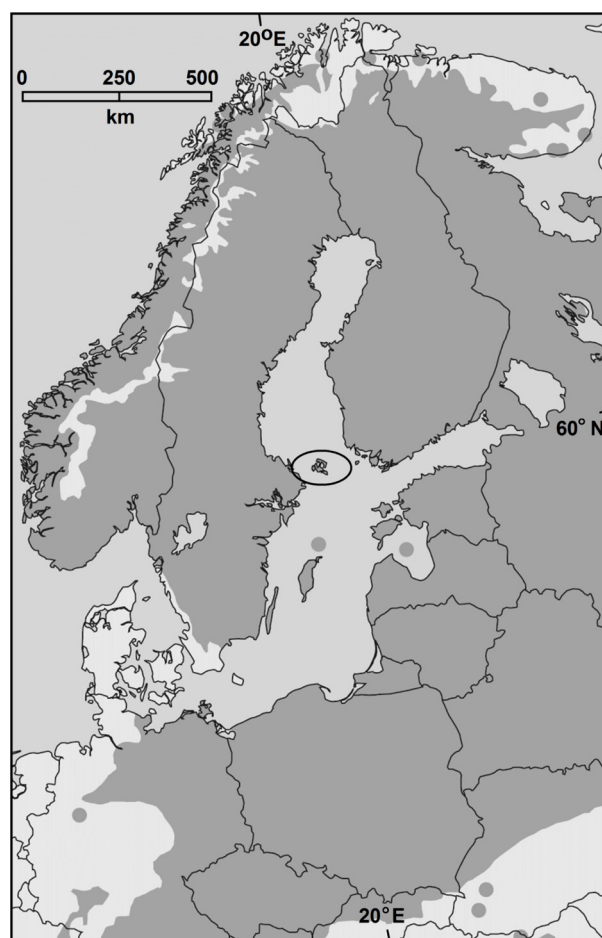


**Fig. 1.** Distribution map of Scots pine, including the Åland Islands (open circle) in Northern Europe. The map was modified following the initial compilation by the members of the EUFORGEN Conifers Network (Mátyás et al. 2004)

structures (Ringbom et al. 1996). These islands form an archipelago in the northern Baltic Sea (ca 60°N, 20°E), south of the Gulf of Bothnia, west of the Gulf of Finland and north of the Baltic Proper, between the mainlands of Finland and Sweden. The Åland archipelago comprises the main island, which is 50 km long (south-north) and 45 km wide (east-west), and about 6500 smaller islands. Annual precipitation totals 553 mm, and the winter (February) and summer (July) temperatures average  $-2.5^{\circ}\text{C}$  and  $15.9^{\circ}\text{C}$ , respectively. The region belongs to the hemiboreal vegetation zone (*sensu* Ahti et al. 1968). The topography of the archipelago is relatively flat, with the exception of rocky areas in the northern and eastern parts. The highest point of Åland reaches 129 m a.s.l. (Autio & Salmela 2010).

Cross-dating of tree-ring data is a dendrochronological procedure that matches ring width variation, especially that of conspicuously wide and narrow rings. Importantly, this procedure can identify the exact calendar years in which the analysed rings formed (Fritts 1976). The tree-ring widths of this study were previously cross-dated (Ringbom et al. 1996). This chronology consists of 111 Scots pine (*Pinus sylvestris* L.) tree-ring series and altogether 11 383 ring width measurements (see Tab. 1). These series were on average 102.5 (median 98) years long. The data comprise a tree-ring chronology covering interval between the years 1057 and 1826. The replication shows considerable variation through time (Fig. 2) and is not continuously covered by any of the nine sites. One of the sites remains undocumented, with no surviving field notes other than that it belongs to the Åland collection of tree-ring data.

### TREE-RING STANDARDIZATION

Age-related components of tree growth were assessed through RCS methods (Helama et al. 2017c). The initial raw tree-ring widths were averaged according to ring number ( $n$ , calculated from the first ring in each tree-ring series). These mean curves displayed the age-dependence in the data and were modelled using a modified negative exponential function (Fritts 1976), following the formula

$$y = ae^{Rn} + y_0 \quad \text{Eq. 1}$$

where parameterization of  $a$ ,  $R$  and  $y_0$  was done by the Levenberg–Marquardt algorithm (Moré 1978). The raw values were divided by the values of the RCS

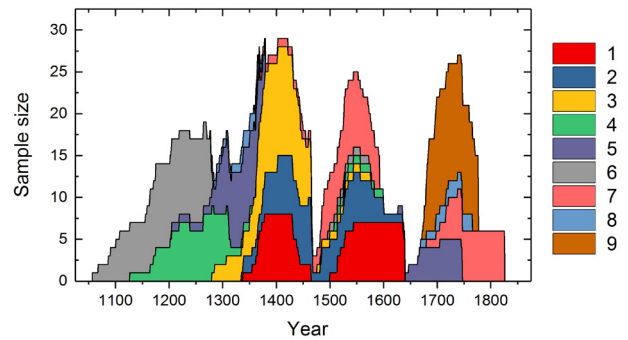


**Fig. 2.** Replication of site-dependent data in the Åland tree-ring chronology. See Table 1 for temporal parameters of site data

curve (Eq. 1) to derive dimensionless tree-ring indices. These index values were realigned according to their cross-dated calendar years and averaged to the mean RCS chronology.

The use of two subgroups representing the data from relatively fast- or slow-growing trees has been recommended as a way to standardize the tree-ring data in these groups by their respective RCS curves (Briffa et al. 2013, Melvin et al. 2013). We applied such multiple RCS curves (MRCS) based on the status (fast- or slow-growing) of the trees, determined from their relative growth rates (RGR) (*sensu* Briffa & Melvin 2011), using the formula

$$RGR = \frac{\sum_{n=1}^{n_{\max}} w_n}{\sum_{n=1}^{n_{\max}} \bar{w}_n} \quad \text{Eq. 2}$$

where  $w_n$  is tree-ring width for ring number  $n$  in the series possessing  $n_{\max}$  tree rings, and  $\bar{w}_n$  is the mean width of all rings for that same ring number (Helama et al. 2012). The age-related curves for both types of trees were averaged and modelled (Eq. 1) separately, and the indices obtained from their respective curves were averaged together to a single mean MRCS chronology.

We also applied a signal-free (SF) approach to the data (Melvin & Briffa 2008) by dividing the values of the initial raw tree-ring width by the values of the mean chronology. The resulting SF series were used to calculate new mean curves according to ring number, and the obtained age-related curves were modelled (using Eq. 1) to derive SF-RCS curves. As was done with the RCS curves, the SF-RCS curves were estimated separately for fast- and slow-growing trees

**Table 1.** Temporal parameters of the Åland site data including the first (FYr) and last (LYr) calendar years of the data, the first (F50) and last (L50) calendar years bracketing the period covered by 50% of the data, the mean (MeanL) and median (MedianL) lengths of the series, and the number of series (N)

n	Site	FYr	LYr	F50	L50	MeanL	MedianL	N
1	Hammarlund	1338	1639	1408	1585	97.8	100	15
2	Eckerö	1335	1635	1416	1539	95.8	93	13
3	Finström	1280	1575	1373	1433	106.9	101	14
4	Lemland	1127	1599	1215	1290	102.3	107.5	10
5	Saltvik	1204	1746	1316	1679	87.8	81	14
6	Jomala	1057	1572	1154	1242	153.5	171	11
7	Geta	1361	1826	1524	1759	99.1	105	16
8	Kumlinge	1278	1765	1341	1728	74.0	79	4
9	Undocumented	1672	1776	1704	1748	88.7	88	14

(using Eq. 2), and new sets of tree-ring indices were calculated to be further averaged into SF-MRCS chronologies. This procedure was repeated five times when the difference between consecutive SF runs at the second decimal place of the mean indices was one or less.

These analyses produced four different mean chronologies (RCS, SF-RCS, MRCS, SF-MRCS), all of them generated from the same initial raw values of ring width. The series of SF-MRCS indices were further detrended using spline functions, with a frequency response of two-thirds of individual series length, and a 50% cut-off (Cook et al. 1990a), and averaged. The resulting detrended index series were further pre-whitened (Cook et al. 1990b) and averaged. These two types of additional chronologies were compared with the RCS chronologies. For visual comparisons, the mean chronologies were smoothed using timescale-dependent cubic smoothing spline functions to illustrate growth variation on multi-decadal and longer scales.

### MULTIPROXY DATASET

In the study region, pine growth variability was expected to reflect variation of summertime precipitation and moisture conditions, as previously demonstrated in areas adjacent to the Åland Islands (Henttonen 1984, Seftigen et al. 2017). Proxy records similarly related to moisture and drought were recently compiled from the mainlands of Finland and Sweden (Linderholm et al. 2018) and were compared here to climate indications inferred from our tree-ring chronology. These data originated from plant macrofossil data recording the peatland water table in Kontolanrahka (60.78°N and 22.78°E) (Väiranta et al. 2007), Cladocera- and chironomid-based records of lake water depth in Iso Lehmälampi (60.33°N and 24.60°E) (Luoto 2009, Nevalainen et al. 2011, Nevalainen & Luoto 2012), and tree accumulation records from lacustrine (61.95°N, 28.97°E) and peatland sites (61.80°N, 29.75°E) in southern Finland (Helama et al. 2017b). Summer moisture conditions (Palmer drought severity index; PDSI) have been reconstructed from a network of moisture-sensitive tree-ring chronologies around Europe, North Africa and the Levant (see Cook et al. 2015 and references therein). Strong anomalies were found for a region of continental Northern Central Europe and Southern Fennoscandia (50–60°N, 5–20°E). The main characteristics of these anomalies were recently found to correspond to the similarly reconstructed PDSI variation for the region of Finland (Helama 2017). We thus compared the Northern Central Europe and Southern Fennoscandia PDSI reconstruction, after the PDSI reconstruction was smoothed using the 100-year cubic smoothing spline function (Cook & Peters 1981) identical to that used to smooth our tree-ring chronologies.

## RESULTS

### AGE-RELATED TRENDS

Averaged according to their ring number, the mean curves of the pine tree-ring width series illustrated notable trends of negative slope and

of exponential shape (Fig. 3a). While the mean ring widths approximated 3 mm near the pith, their subsequent narrowing to an average ca 1 mm after the first 50 years was clearly demonstrated. There was replication of at least ten tree-ring series over the first 150 years, at which age the mean ring widths approximated 0.4 mm. Similar findings were shown for the data also after implementation of the signal-free approach, indicating that the described changes in the mean curves likely originate mainly from age-dependent factors in tree growth. The fast- and slow-growing trees seemed to exhibit an age-related change of exponential shape, yet their overall growth levels were found to differ markedly (Fig. 3b). While the fast-growing trees had rings nearly 1 mm wider on average near the pith, the difference was decreased to ca 0.2 mm at age of 100 years.

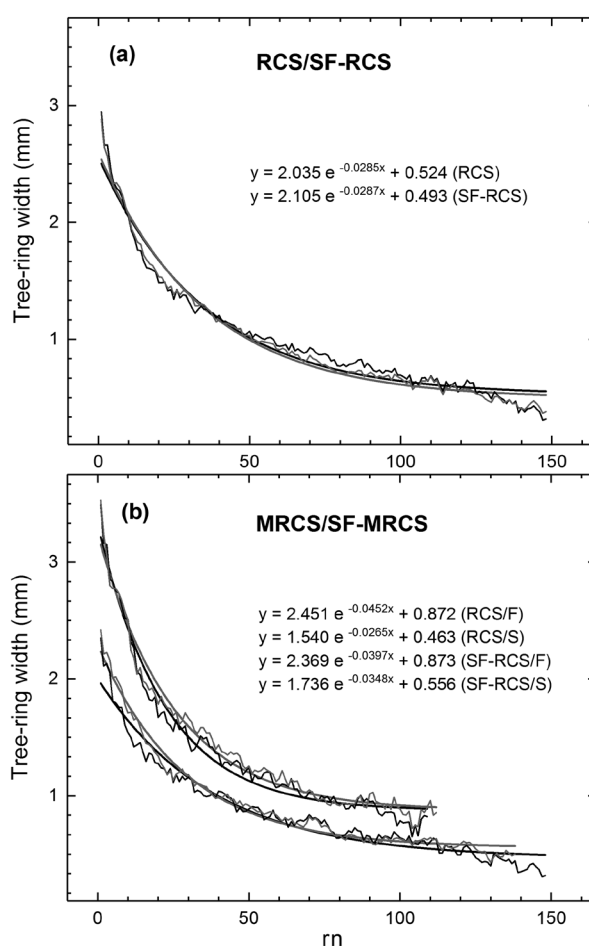


**Fig. 3.** Mean age-dependent change in the tree-ring series as a function of ring number (rn) estimated for pine tree-ring width data from the Åland Islands using regional curve standardization with single (RCS; black lines) (a) and multiple (MRCS; black lines) curves (b) and with signal-free (SF-RCS/SF-MRCS; grey lines) implementation, separately for fast-growing (F) and slow-growing (S) trees (b), each model (Eq. 1) being applied for mean values with at least ten trees

## SITE-DEPENDENT GROWTH

Age-related mean curves of similar shape were obtained for each of the sites. Comparison of the mean curves calculated from the tree-ring widths (Fig. 4a) and the SF series (Fig. 4b) showed that the curves of the former type were spread over a considerably wider range of growth levels. In other words, the curves computed from the SF series became surprisingly uniform in their growth variation, and the mean curves meandered around each other. These findings were reproduced in the analysis of the modelled growth. When the exponential function (Eq. 1) was used to model the mean curves, the tree-ring widths before SF implementation did indicate a notably wider range of growth levels between the sites (Fig. 4c), as compared to the curves modelled using the SF series (Fig. 4d). These results suggest the benefit of the SF approach in removing climatic

effects from the initial ring width data before standardization of the series. Considering that the different sites were composed of tree-ring data representing different time intervals, and of different climate periods, the wider spread of the initial data (Fig 4a, c) may be expected to largely originate from the climatic signal, which is then removed from the data during SF implementation (Fig. 4b, d).

Similar findings were evident for the relative growth rates (RGR). Before SF implementation, five out of nine sites showed mean RGR above the overall mean; four sites had mean RGR below that level (Tab. 2). The differences between the site-dependent and overall RGR means were found to be statistically significant ( $t$ -test,  $p < 0.05$ ) for sites 4 and 6, for which the site-dependent RGRs remained below the mean value. Consistently, both the observed and modelled age-related growth curves could be seen to be lower at these two sites than at the other

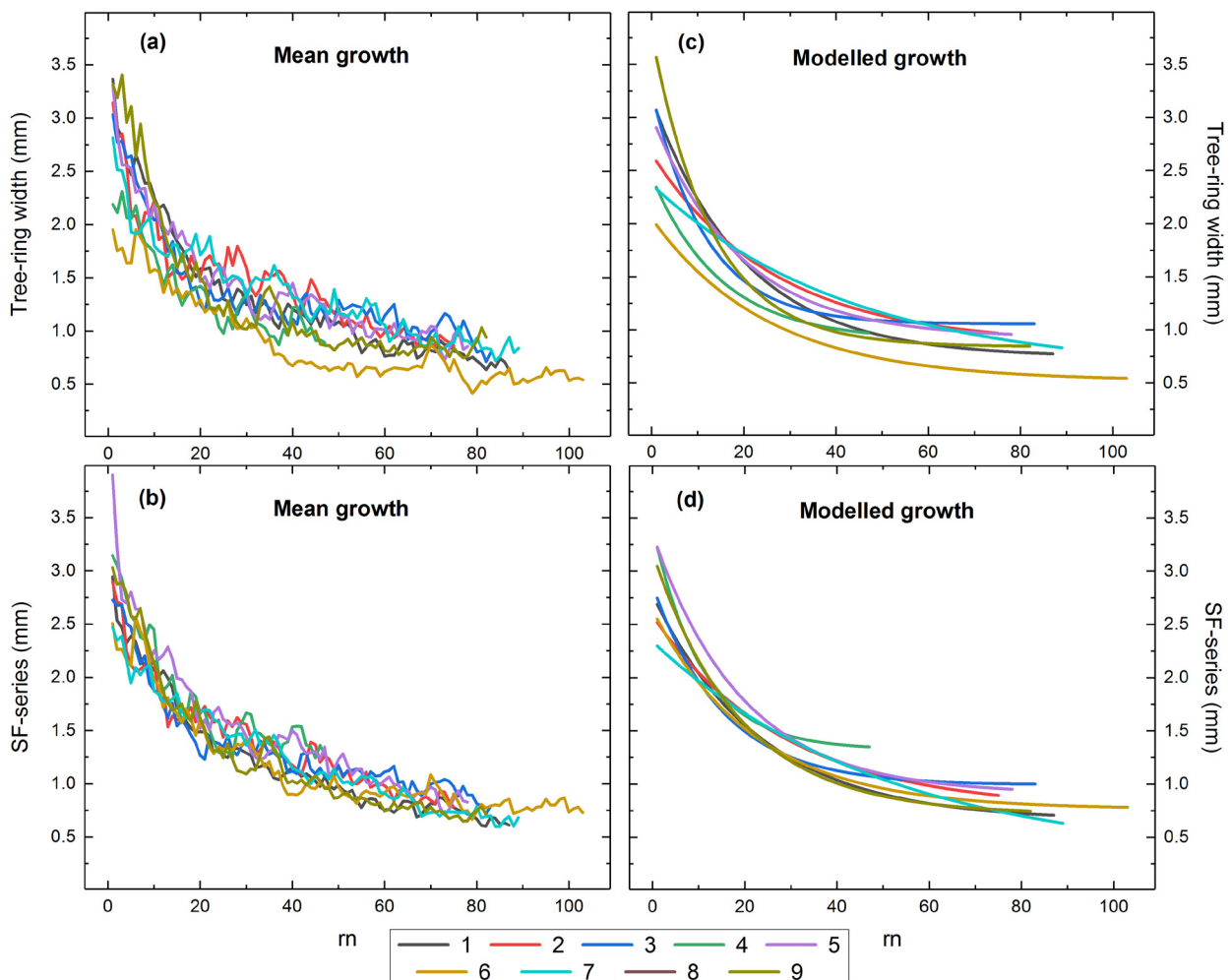


**Fig. 4.** Mean age-dependent change for the different sites (1–9) calculated from tree-ring width (a) and the signal-free (SF) series (b), and modelled using the predetermined function (Eq. 1) for the mean records (c, d), as a function of ring number (rn). See Table 1 for temporal parameters of site data

sites (see Fig. 4a, c). For the SF series, four out of nine sites had their mean RGRs below the overall mean, and five sites below that level. For these data, sites 4 and 6 were no longer found to show a significant ( $p > 0.05$ ) difference from the overall RGR level. Similar results were evident for the growth curves obtained from the SF series (see Fig. 4b, d), for which sites 4 and 6 were not anomalous. Instead, site 1 had its mean RGR differing significantly ( $t$ -test,  $p < 0.05$ ) from that level, remaining above the overall mean RGR value.

#### MEAN CHRONOLOGIES

Age-related changes in radial growth were modelled using negative exponential functions fitted to each of the mean curves. These components of radial growth represented the resulting RCS curves that were further removed from the individual tree-ring series by dividing the observations of raw data by the values of their respective RCS curves. The resulting RCS chronologies showed markedly variable growth over the study period. The RCS and SF-RCS chronologies agreed especially in their short- and long-term variability (Fig. 5a). The tree-ring indices remained below 1.0 over most of the first two centuries of the study period, and above that level after the mid-18<sup>th</sup> century. No such long-term growth perturbations were evident over the intermediate period, from the 14<sup>th</sup> to 18<sup>th</sup> centuries, when both the RCS and SF-RCS chronologies displayed index values of around 1.0.

These long-term changes were somewhat attenuated when a new set of chronologies was generated (Fig. 5b) by standardizing the fast- and slow-growing trees by their respective MRCS curves. While especially the early part of the MRCS chronology had index values approaching those of the intermediate period, the SF-MRCS chronology was seen to exhibit somewhat lower values over these early centuries. Over the post-1750 period, both the MRCS and SF-MRCS chronologies did indicate a positive growth phase, though less distinct than in the RCS and SF-RCS chronologies. Although the four tree-ring chronologies were generally very similar in their characteristics, their long-term growth estimates were clearly differentiated following SF implementation and the use of either one (RCS) or two (MRCS) curves to standardize the raw tree-ring series.

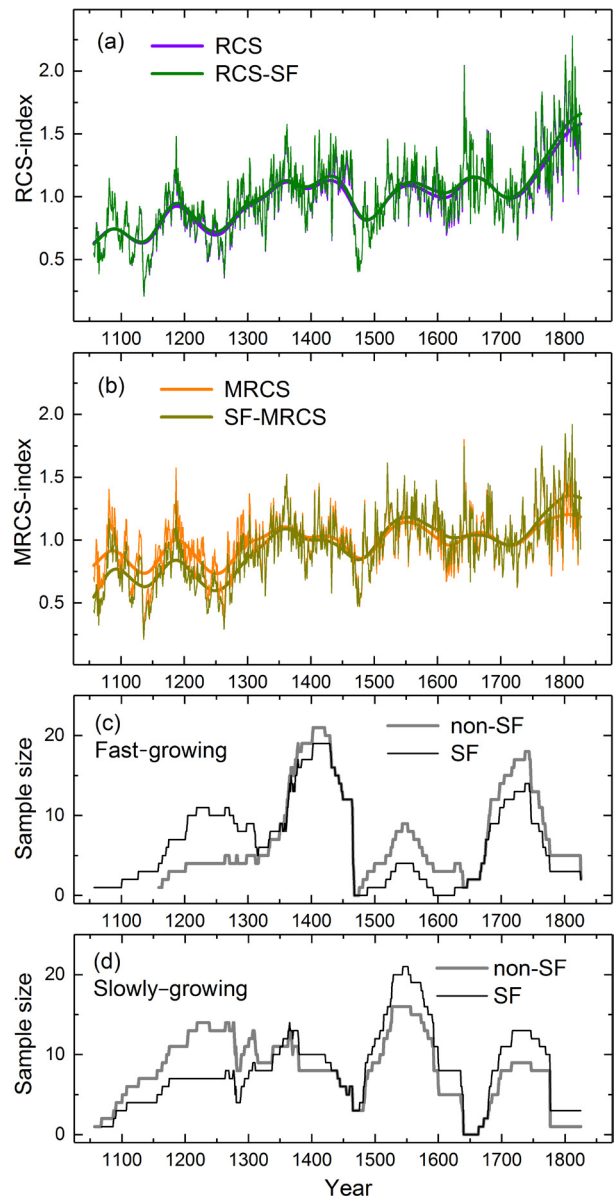


**Fig. 5.** Tree-ring chronologies produced using regional curve standardization with single (RCS) (a) and multiple (MRCS) (b) curves and with signal-free (SF-RCS) implementation, illustrated for their annual (thin lines) and long-term (thick lines) variation. The long-term component of growth variability was isolated using a 100-year spline function. Replication of fast-growing (c) and slow-growing (d) trees based on tree-ring width series (non-SF) and signal-free (SF) series

The post-1750 growth phase appeared to be mainly occupied by fast-growing trees (Fig. 5c). Standardizing these series using their respective MRCS/SF-MRCS curves (see Fig. 3b) did obviously lower their resulting tree-ring index values over the same period (Fig. 5b) as compared with the RCS/SF-RCS chronologies (Fig. 5a). This effect appeared to be similar for the MRCS/SF-MRCS indices. Quite a different effect was observed over the first centuries (prior to 1250), however. Comparing the chronological positions of fast- or slow-growing trees, it becomes apparent that the deviations

in tree-ring indices over this period may actually result from changes caused by the SF implementation for tree status estimated as either fast- or slow-growing. First, there were few if any changes in these positions since the mid-14<sup>th</sup> century, that is, the period over which the MRCS and SF-MRCS chronologies appeared not to differ markedly (see Fig. 5c, d). Second, the relatively high number of trees judged as slow-growing, observed here until the mid-14<sup>th</sup> century before SF implementation, was changed to a similarly higher number of trees with fast-growing status after the implementation. Since the raw values of those tree-ring data are then to be divided by the values of the SF-MRCS curve of fast- rather than slow-growing trees (see Fig. 3b), and thus by the curve with higher expected growth values, the resulting mean indices may, as a consequence, reach considerably lower values over the same period (i.e. prior to 1250).

Obviously, the SF-MRCS approach was able to deal with issues in the structure of the data.

Indices of this type are used in the following section to further analyse the climatic signals in the Åland tree-ring chronology. As compared to this chronology, the mean chronology resulting from the spline detrending procedure contained much less low-frequency growth variability (Fig. 6a, b). Moreover, the mean chronology produced after the tree-ring series were pre-whitened could be found to be even weaker in that respect (Fig. 6c). Although these chronologies could not be used to estimate the long-term growth and climatic variation, it is evident that their multi-decadal to sub-centennial fluctuations did in fact correspond with those of the RCS chronologies. That is, the phases of low growth coincided in the different chronologies over most of the first two centuries of the study period, especially around the mid-12<sup>th</sup> century and over the first half of the 13<sup>th</sup> century, around 1500, and over the early decades of the 17<sup>th</sup> century (Fig. 6d). Coinciding phases of higher growth were evident around the mid-14<sup>th</sup> and mid-17<sup>th</sup> centuries.

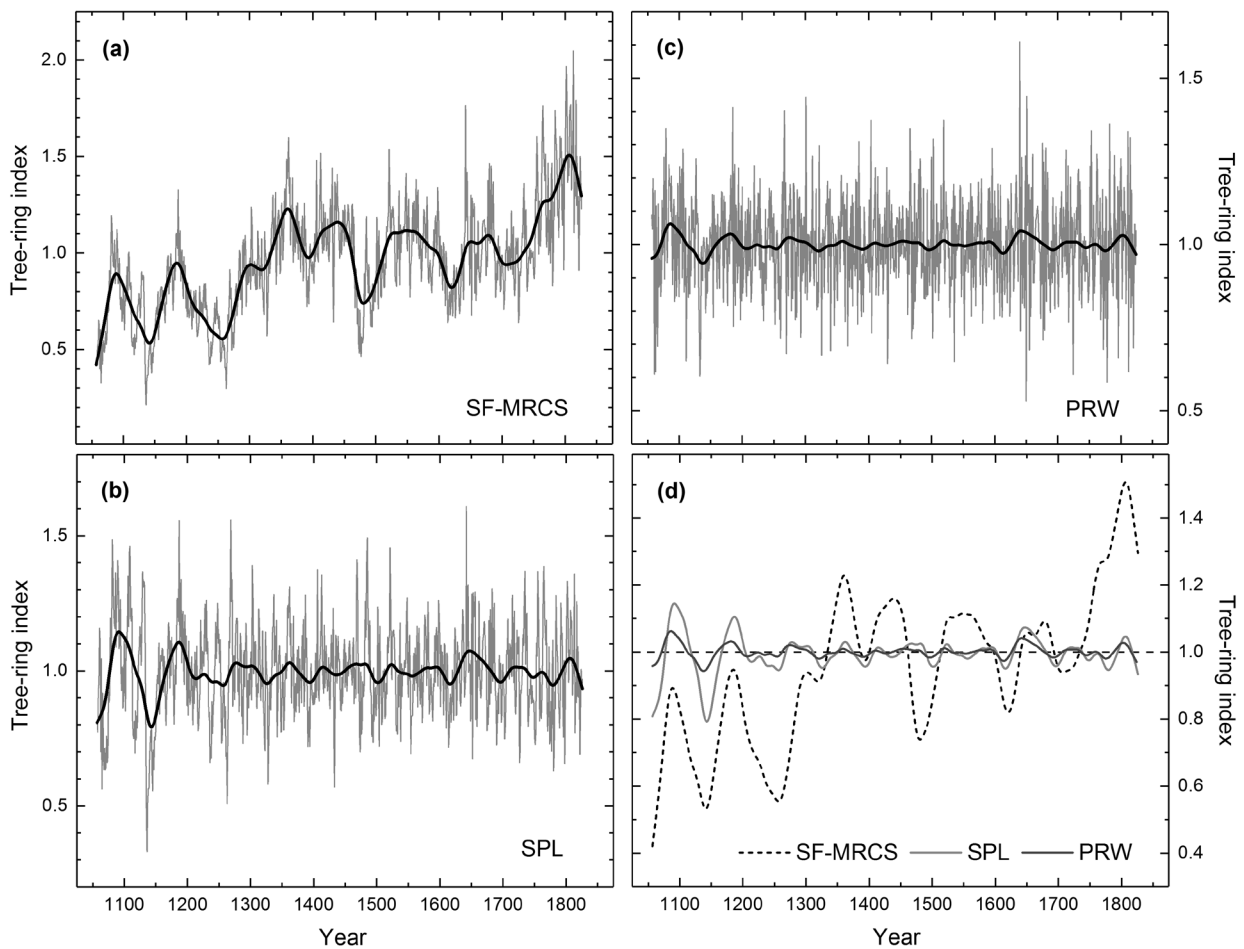


**Fig. 6.** Tree-ring chronologies produced using regional curve standardization with multiple curves and with signal-free (SF-MRCS) implementation (a), spline detrending (SPL) (b) and pre-whitening (PRW) (c) illustrated for their annual (thin line) and long-term (thick line) variation. The long-term component of growth variability was isolated using a 50-year spline function (d)

## MULTI-PROXY COMPARISON

A feature common to the multi-proxy records was their indication of reduced moisture roughly over the pre-1250 period, as implied by the lower peatland water table and lake water depth, and by the reduced Palmer drought severity index (PDSI) in the corresponding reconstructions (Fig. 7). Similar indications were obtained from the depositional histories of pine trees, which reflected increasing accumulation of peatland trees around 1000, with indication of dry surface conditions (see Helama et al. 2017b). Moreover, a peak in lakeside tree accumulation was evident towards the late 13<sup>th</sup> century, potentially indicating rising lake levels, similar to lake level reconstructions derived from microfossil assemblages. Our SF-MRCS chronology agreed with the general long-term changes in other proxy records, demonstrating the usefulness of the Åland chronology for inferring past variation of climate conditions in the region.

An additional feature common to several proxy records was the indication of an at least multi-decadal dry period around the mid-15<sup>th</sup> century, and an increase in moisture since that event. This event could be found in a chironomid-based reconstruction of lake water depth and tree-ring based reconstructions of the PDSI, in addition to our chronology (Fig. 7). Moreover, these changes could be related to a transient reduction of lakeside tree accumulation and to a slight increase of their accumulation thereafter and towards the early 16<sup>th</sup> century. The positive trend in the SF-MRCS chronology over its most recent decades did not agree with other proxy records. Over this period, however, the chronology was replicated by fewer tree-ring series, suggesting that its ability to indicate past climatic variation during this interval may be suboptimal.

## DISCUSSION AND CONCLUSIONS

The tree-ring records from the Åland Islands were shown to provide proxy data comparable with previously published sedimentary and tree-ring evidence. The main focus of this paper was on tree-ring data produced using regional curve standardization (RCS) (Briffa et al. 1992, 1996, Briffa & Melvin 2011, Helama et al. 2017c). The choice of a tree-ring standardization method is known to affect the properties

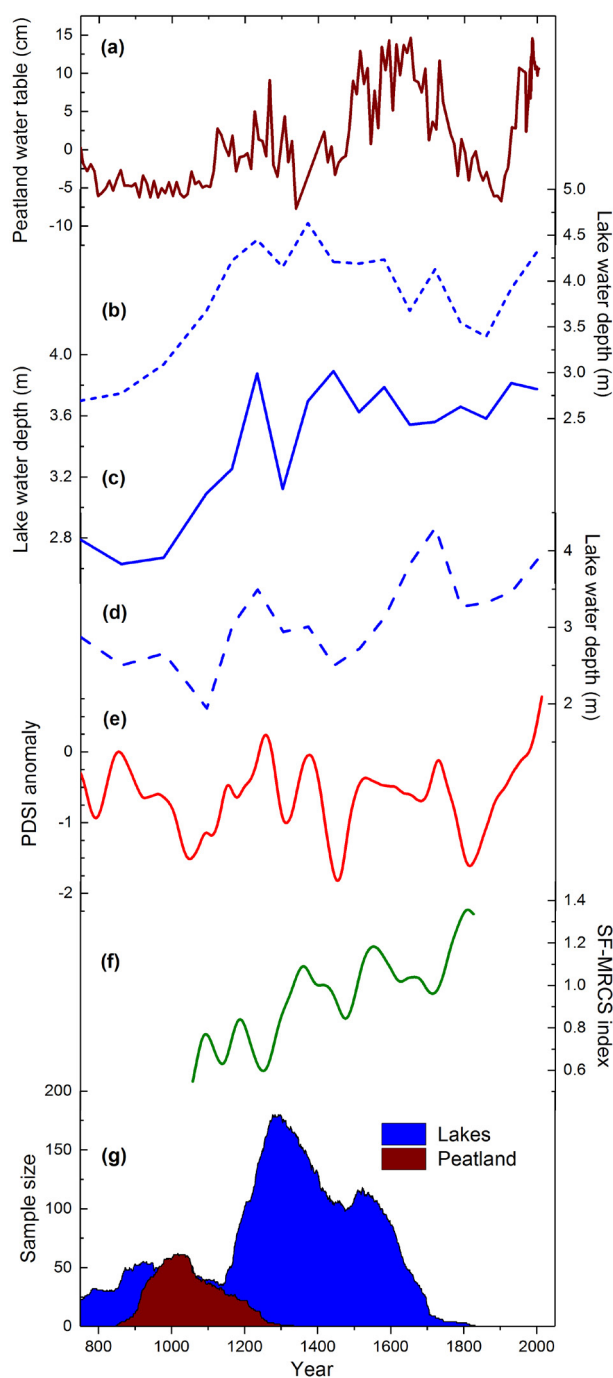


**Fig. 7.** Multiproxy comparison including the plant macrofossil record of the peatland water table (Väliranta et al. 2007) (a), Cladocera-based records of lake water depth (Nevalainen & Luoto 2012) (b) and (Nevalainen et al. 2011) (c), chironomid-based records of lake water depth (Luoto 2009) (d), tree-ring-based records of the Palmer drought severity index (PDSI) (Cook et al. 2015) (e), our SF-MRCS chronology (f), and tree accumulation records from south-eastern Finland (Helama et al. 2017b) (g)

of the resulting chronology and especially to modify their low-frequency variability. In short, the chronologies produced using the RCS method are expected to retain the growth variation at wavelengths exceeding the lengths of the individual tree-ring series constituting the chronology (Cook et al. 1995). Therefore, the

use of non-RCS methods to standardize raw tree-ring series could impair comparisons of tree-ring and other proxy records that may not show short-term variation due simply to the lack of high-resolution data in many sedimentary records. This was largely the case for our tree-ring data, as the chronologies produced by spline detrending (i.e. non-RCS procedure) did not show low-frequency growth variation comparable to that produced using the RCS procedure (Fig. 6). In any case, the RCS and non-RCS chronologies showed notable similarities in their multi-decadal and sub-centennial variation, at least over certain periods of high and low growth index values, clearly indicating that the growth anomalies in the RCS chronologies were not simply products of data heterogeneity, to which the RCS procedure is more sensitive than non-RCS methods (Briffa & Melvin 2011). Indeed, the Åland chronology is characterized by conspicuous fluctuation of the number of available samples through time (Fig. 2). We note that this fluctuation may be an unavoidable feature of the sample material, as church-building activity may have been inherently related to changing environmental constraints that generally affected the contemporary population's tax-paying ability over historical time (Holopainen et al. 2016).

Here, the use of RCS methods helped us to unveil the centennial and longer variation in the Åland tree-ring dataset and to compare the obtained growth variation with hydroclimate variation reconstructed from other types of proxy data. The use of RCS and SF-RCS methods did not result in markedly altered low-frequency estimates of tree growth (Fig. 5a), whereas the MRCS and SF-MRCS chronologies differed more (Fig. 5b). In terms of relative growth rates (RGRs; Tab. 2), sites 4 and

6 showed lower growth values than the other sites; on the other hand, these were the sites that dominated the chronology over its first centuries (Fig. 2), when tree growth could indeed have been reduced by drought, as shown by other proxy records. This could be deduced from plant macrofossil (Väliranta et al. 2007), Cladocera and chironomid records (Luoto 2009, Nevalainen et al. 2011, Nevalainen & Luoto 2012) indicating that southern Finland was under persistent drought, resulting in lower peatland water table and lake water depths (Fig. 7). When this signal of climatic origin was taken into account in assessing the RCS curves, through SF implementation, the corresponding sites did not exhibit similarly anomalous RGRs (Tab. 2). Collectively, these results would demonstrate a specific effect: that SF implementation removed the climate signal from the raw data in this case, after which the use of SF-MRCS curves to standardize the tree-ring data showed the advantage of restoring that signal in our SF-MRCS chronology.

Previous studies have shown that Scots pine radial growth is related to variation of warm-season precipitation and moisture conditions when analysed at similar latitudes in Northern Europe (Henttonen 1984). These chronologies have been used as proxy data sources for reconstruction of corresponding climatic factors, as demonstrated for various sites and regions in Sweden (Linderholm & Molin 2005, Jönsson & Nilsson 2009, Seftigen et al. 2013) and Finland (Helama & Lindholm 2003, Helama et al. 2009, Helama 2014), and for greater Fennoscandia using a network of moisture-sensitive tree-ring chronologies (Seftigen et al. 2015). Our data did not overlap with the period of modern instrumental weather observations for the Åland Islands (Tuomenvirta et al. 2001).

**Table 2.** Comparison of relative growth rates, including the number of the site ( $n$ ; see Table 1), the site-dependent averages before (RGR) and after ( $RGR_{sf}$ ) signal-free implementation, the mean of all series excluding the particular site before ( $RGR_{all}$ ) and after signal-free implementation ( $RGR_{all-sf}$ ), the difference between RGR and  $RGR_{all}$  (Diff1), with the significance of the  $t$ -test ( $p$  (1)) to compare means, and the difference between  $RGR_{sf}$  and  $RGR_{all-sf}$  (Diff2), with the significance of the  $t$ -test ( $p$  (2)) to compare means

$n$	RGR	$RGR_{sf}$	$RGR_{all}$	$RGR_{all-sf}$	Diff1	$p$ (1)	Diff2	$p$ (2)
1	1.000	0.920	1.023	1.024	-0.023	0.580	-0.104	0.026
2	1.117	1.046	1.007	1.005	0.110	0.229	0.041	0.601
3	1.052	0.998	1.015	1.011	0.037	0.377	-0.013	0.746
4	0.869	1.113	1.034	0.999	-0.165	0.011	0.114	0.204
5	1.060	1.080	1.014	0.999	0.046	0.378	0.081	0.144
6	0.769	0.967	1.047	1.014	-0.278	0.001	-0.047	0.577
7	1.102	0.974	1.006	1.016	0.096	0.168	-0.042	0.440
8	1.327	1.263	1.008	1.000	0.319	0.066	0.263	0.095
9	1.000	0.941	1.022	1.019	-0.022	0.609	-0.078	0.078

We note, however, that historical precipitation observations (1749–1800) from Turku, southwestern Finland (Holopainen 2004, 2006), do overlap with the most recent part of our tree-ring data. Correlating the Åland tree-ring chronology with the monthly precipitation records of this historical dataset demonstrates strong relationships ( $r \sim 0.5$ ) with the spring and summer precipitation records (Fig. 8). The correlations were highest for June and for March through August. As a caveat, the Åland chronology is not sufficiently replicated over this period, especially since 1777 (see Fig. 2); more tree-ring series would be needed to ascertain this climate–growth relationship. Moreover, Turku is on the Finnish mainland, so it may not fully represent climate conditions on the Åland Islands. Nor are we certain that the historical observations of precipitation can yield climate–growth correlations as reliably as modern climate data can. These faults notwithstanding, the relationships between the warm-season

precipitation and pine radial growth are appreciably strong ( $r \sim 0.5$ ). The results of this correlation analysis also largely agree with the relationships found in previous tree-ring studies from different sites on the mainlands of Sweden and Finland. It seems fairly safe to assume that similar climate–growth relationships probably controlled pine radial growth on the Åland Islands, as recorded by the RCS chronologies of this study.

As previously alluded to, the low-frequency connections between the proxy records agreed in indicating dry conditions over the pre-1250 period. Another dry period was found around the mid-15<sup>th</sup> century (Fig. 7). Both of these indications were in accord with the previously developed *Old World Drought Atlas* (OWDA), which is a series of year-to-year maps of gridded, tree-ring-based reconstructions of summer wetness and dryness over Europe and the Mediterranean Basin (Cook et al. 2015). These droughts were observed as an average of the

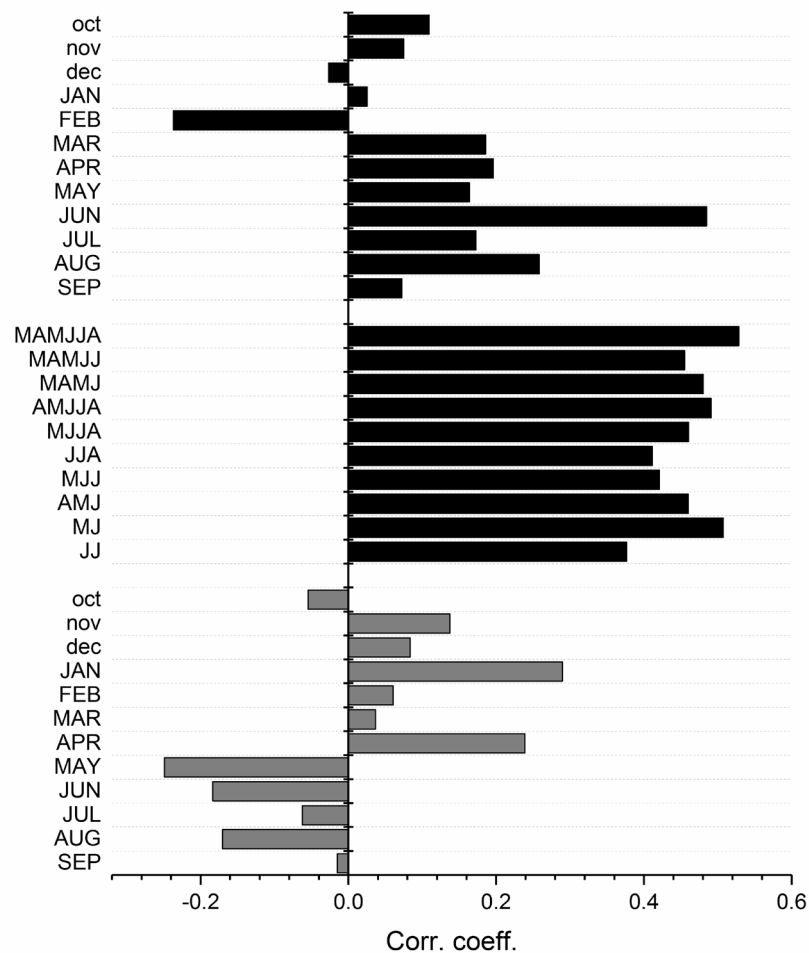


**Fig. 8.** Pearson correlations between the Åland tree-ring chronology and historical climate records from Turku (Holopainen 2004). The mean chronology of pre-whitened tree-ring indices was compared with the monthly and seasonal precipitation sums (black histograms) and monthly mean temperatures (grey histograms) of the previous (small letters) and concurrent year (capital letters). Correlations were calculated over the 1751–1800 period

OWDA reconstructions for Northern Central Europe and Southern Fennoscandia, which form an area partly overlapping the Åland Islands. There were no tree-ring data from the Åland Islands in the OWDA dataset used in that summer soil moisture reconstruction (see Cook et al. 2015), so our tree-ring records add palaeoclimate information for geographical areas where similar data are not currently available. Our results reinforce these findings and demonstrate that the northern reach of the droughts likely extended over the Åland Islands. We also note that the drought reconstructed for Northern Central Europe from the OWDA dataset for the period from 1779 to 1827 (Cook et al. 2015) did not appear in our tree-ring records. Previously, an overlapping dry period was inferred from tree-ring and documentary data for a shorter period from 1815 to 1833 in eastern central Sweden (Linderholm & Molin 2005), for a period from the mid-1800s to early 1830s in south-eastern Sweden (Seftigen et al. 2013) and from around the same time in south-eastern Finland (Helama et al. 2009) and, albeit much less pronounced, in western Estonia (Helama et al. 2018). In any case, the sample replication of our chronology was not high enough to allow any definitive conclusions to be drawn for that period.

An analysis by Läänelaid et al. (2012) showed that the Åland tree-ring data correlated positively with other Scots pine tree-ring chronologies from Estonia, Finland, Sweden, Lithuania, Poland and north-western Russia. Their comparison began with the 12<sup>th</sup> century. The strength of their inter-chronological correlations varied, with the strongest correlations between chronologies being found for periods with enhanced winter westerlies (Trouet et al. 2009); these winds bring mild, moist Atlantic air masses onto the region (Hurrell 1995). These associations suggest that, in addition to the precipitation signal, the Åland chronology may contain a climatic signal of winter climate, at least that of temperature. Supporting this, a comparison with the historical weather observations from Turku show the highest (positive) temperature correlation ( $r \sim 0.3$ ) with mean January temperature (Fig. 8). Clearly there is a need to collect a representative set of living tree samples from the Åland Islands for a critical evaluation of the dendroclimatic signals over the period when climatic variation has been instrumentally observed in the

region. Such an analysis can not only determine the climatic factors governing pine radial growth in the Åland Islands but also detail the regional variability of climate–growth relationships across the archipelago.

#### ACKNOWLEDGEMENTS

The authors thank Professor Å. Ringbom for her help with the data and publications, and Dr K.-U. Heußner and an anonymous reviewer for their comments, which improved the manuscript. This paper was written while the first author was supported by a grant (no. 288267) from the Academy of Finland.

#### REFERENCES

- AHTI T., HÄMET-AHTI L. & JALAS J. 1968. Vegetation zones and their sections in northwestern Europe. *Ann. Bot. Fennici*, 3: 169–211
- AUTIO O. & SALMELA J. 2010. The semi-aquatic fly fauna (Diptera) of wetlands of the Åland Islands. *Memoranda Soc. Fauna Flora Fennica*, 86: 43–53.
- BALANZATEGUI D., KNORR A., HEUSSNER K.-U., WAZNY T., BECK W., SŁOWIŃSKI M., HELLE G., BURAS A., WILMKING M., VAN DER MAATEN E., SCHARNWEBER T., DORADOLINÁN I. & HEINRICH I. 2018. An 810-year history of cold season temperature variability for northern Poland. *Boreas*, 47: 443–453.
- BRIFFA K.R. & MELVIN T.M. 2011. A closer look at Regional Curve Standardization of tree-ring records: Justification of the need, a warning of some pitfalls, and suggested improvements of its application: 113–145. In: Hughes M.K., Diaz H.F. & Swetnam T.W. (eds), *Dendroclimatology: Progress and Prospects*. Springer Verlag, Berlin.
- BRIFFA K.R., JONES P.D., BARTHOLIN T.S., ECKSTEIN D., SCHWEINGRUBER F.H., KARLEN W., ZETTERBERG P., ERONEN M. 1992. Fennoscandian summers from AD 500: temperature changes on short and long timescales. *Clim. Dyn.*, 7: 111–119.
- BRIFFA K.R., JONES P.D., SCHWEINGRUBER F.H., KARLEN W. & SHIYATOV S.G. 1996. Tree-ring variables as proxy-climate indicators: Problems with low-frequency signals: 9–41. In: Jones P.D., Bradley R.S. & Jouzel J. (eds), *Climate variations and forcings mechanisms of the last 2000 years*. Springer, Berlin.
- BRIFFA K.R., MELVIN T.M., OSBORN T.J., HANTEMIROV R.M., KIRDYANOV A.V., MAZEPA V.S., SHIYATOV S.G. & ESPER J. 2013. Reassessing the evidence for tree-growth and inferred temperature change during the Common Era in Yamalia, north-west Siberia. *Quaternary Sci. Rev.*, 72: 83–107.
- COOK E.R. & PETERS K. 1981. The smoothing spline: a new approach to standardizing forest interior tree-ring width series for dendroclimatic studies. *Tree-Ring Bull.*, 41: 45–53.

- COOK E.R., BRIFFA K.R., MEKO D.M., GRAYBILL D.A. & FUNKHOUSER G. 1995. The 'segment length curse' in long tree-ring chronology development for paleoclimatic studies. *Holocene*, 5: 229–237.
- COOK E., BRIFFA K., SHIYATOV S., MAZEPA V. 1990a. Tree-ring standardization and growth-trend estimation: 104–123. In: Cook E.R. & Kairiukstis L.A. (eds), *Methods of Dendrochronology: Applications in the Environmental Sciences*. Kluwer Academic Publishers, Dordrecht.
- COOK E.R., SEAGER R., KUSHNIR Y., BRIFFA K.R., BÜNTGEN U., FRANK D., KRUSIC P.J., TEGEL W., VAN DER SCHRIER G., ANDREU-HAYLES L., BAILLIE M., BAITTINGER C., BLEICHER N., BONDE N., BROWN D., CARRER M., COOPER R., ČUFAR K., DITTMAR C., ESPER J., GRIGGS C., GUNNARSON B., GÜNTHER B., GUTIERREZ E., HANECA K., HELAMA S., HERZIG F., HEUSSNER K.-U., HOFMANN J., JANDA P., KONTIC R., KÖSE N., KYNCL T., LEVANIČ T., LINDERHOLM H., MANNING S., MELVIN T.M., MILES D., NEUWIRTH B., NICOLUSSI K., NOLA P., PANAYOTOV M., POPA I., ROTHE A., SEFTIGEN K., SEIM A., SVARVA H., SVOBODA M., THUN T., TIMONEN M., TOUCHAN R., TROTSIUK V., TROUET V., WALDER F., WAŻNY T., WILSON R. & ZANG C. 2015. Old World megadroughts and pluvials during the Common Era. *Science Adv.*, 1: DOI: 10.1126/sciadv.1500561.
- COOK E., SHIYATOV S. & MAZEPA V. 1990b. Estimation of the mean chronology: 123–132. In: Cook E.R. & Kairiukstis L.A. (eds), *Methods of Dendrochronology: Applications in the Environmental Sciences*. Kluwer Academic Publishers, Dordrecht.
- COOPER R.J., MELVIN T.M., TYERS I., WILSON R.J.S. & BRIFFA K.R. 2013. A tree-ring reconstruction of East Anglian (UK) hydroclimate variability over the last millennium. *Clim. Dyn.*, 40: 1019–1039.
- FRITTS H.C. 1976. *Tree rings and climate*. New York, Academic Press.
- HELAMA S. 2014. The Viking Age as a Period of Contrasting Climatic Trends: 117–130. In: Ahola J., Frog & Tolley C. (eds), *Fibula, Fabula, Fact. Defining and Contextualizing the Viking Age in Finland*. Finnish Literature Society.
- HELAMA S. 2017. An overview of climate variability in Finland during the Common Era. *Geophysica*, 52: 3–20.
- HELAMA S. & LINDHOLM M. 2003. Droughts and rainfall in south-eastern Finland since AD 874, inferred from Scots pine ring-widths. *Bor. Environm. Res.*, 8: 171–183.
- HELAMA S., HUHTAMAA H., VERKASALO E. & LÄÄNELAID A. 2017a. Something old, something new, something borrowed: New insights to human-environment interaction in medieval Novgorod inferred from tree rings. *J. Archaeol. Sci. Reports*, 13: 341–350.
- HELAMA S., LÄÄNELAID A., RAISIO J. & TUOMENVIRTA H. 2012. Mortality of urban pines in Helsinki explored using tree rings and climate records. *Trees*, 26: 353–362.
- HELAMA S., MERILÄINEN J., TUOMENVIRTA H. 2009. Multicentennial megadrought in northern Europe coincided with a global El Niño–Southern Oscillation drought pattern during the Medieval Climate Anomaly. *Geology*, 37: 175–178.
- HELAMA S., LUOTO T.P., NEVALAINEN L. & EDVARDSSON J. 2017b. Rereading a tree-ring database to illustrate depositional histories of sub-fossil trees. *Palaeontol. Electron.*, 20(1): 1–12.
- HELAMA S., MELVIN T.M. & BRIFFA K.R. 2017c. Regional curve standardization: State of the art. *Holocene*, 27: 172–177.
- HELAMA S., SOHAR K., LÄÄNELAID A., BIJAK S. & JAAGUS J. 2018. Reconstruction of precipitation variability in Estonia since the 18th century, inferred from oak and spruce tree rings. *Clim. Dyn.*, 50: 4083–4101.
- HENTTONEN H. 1984. The dependence of annual ring indices on some climatic factors. *Acta Forestalia Fennica*, 186: 1–38.
- HOLOPAINEN J. 2004. Turun varhainen ilmastollinen havaintosarja [The early climatological records of Turku, in Finnish]. *Finnish Meteorological Institute/Meteorological Research* 2004(8): 1–54.
- HOLOPAINEN J. 2006. Reconstructions of past climates from documentary and natural sources in Finland since the 18th century. *Publ. Dept. Geol. Univ. Helsinki*, D9: 1–33.
- HOLOPAINEN J., HELAMA S. & HUHTAMAA H. 2016. An environmental historical view of unfinished medieval stone churches. *Society for Medieval Archaeology in Finland Journal SKAS* 1/2016: 3–10.
- HUGHES M.K. 2011. Dendroclimatology in high-resolution paleoclimatology: 17–34. In: Hughes M.K., Swetnam T.W. & Diaz H.F. (eds). *Dendroclimatology. Developments in Paleoenvironmental Research* 11. Springer, Dordrecht.
- HURRELL J.W. 1995. Decadal trends in the North Atlantic oscillation: regional temperatures and precipitation. *Science*, 269: 676–679.
- JÖNSSON K. & NILSSON C. 2009. Scots pine (*Pinus sylvestris* L.) on shingle fields: a dendrochronologic reconstruction of early summer precipitation in mideast Sweden. *J. Clim.*, 22: 4710–4722.
- KOPROWSKI M., PRZYBYLAK R., ZIELSKI A. & POSPIESZYŃSKA A. 2012. Tree rings of Scots pine (*Pinus sylvestris* L.) as a source of information about past climate in northern Poland. *Int. J. Biometeorol.*, 56: 1–10.
- LÄÄNELAID A., HELAMA S., KULL A., TIMONEN M. & JAAGUS J. 2012. Common growth signal and spatial synchrony of the chronologies of tree-rings from pines in the Baltic Sea region over the last nine centuries. *Dendrochronologia*, 30: 147–155.
- LINDERHOLM H.W. & MOLIN T. 2005. Early nineteenth century drought in east central Sweden inferred from dendrochronological and historical archives. *Clim. Res.*, 29: 63–72.

- LINDERHOLM H.W., NICOLLE M., FRANCUS P., GAJEWSKI K., HELAMAS., KORHOLA A., SOLOMINA O., YU Z., ZHANG P., D'ANDREA W.J., DEBRET M., DIVINE D.V., GUNNARSON B.E., LOADER N.J., MASSEI N., SEFTIGEN K., THOMAS E.K., WERNER J., ANDERSSON S., BERNTSSON A., LUOTO T.P., NEVALAINEN L., SAARNI S. & VÄLIRANTA M. 2018. Arctic hydroclimate variability during the last 2000 years: current understanding and research challenges. *Clim. Past*, 14: 473–514.
- LUOTO T.P. 2009. A Finnish chironomid- and chao-borid-based inference model for reconstructing past lake levels. *Quatern. Sci. Rev.*, 28: 1481–1489.
- LUOTO T.P. & NEVALAINEN L. 2018. Temperature-precipitation relationship of the Common Era in northern Europe. *Theor. Appl. Climatol.*, 132: 933–938.
- MÁTYÁS C., ACKZELL L. & SAMUEL C.J.A. 2004. EUFORGEN technical guidelines for genetic conservation and use for Scots pine (*Pinus sylvestris*). Rome, International Plant Genetic Resources Institute.
- MELVIN T.M. & BRIFFA K.R. 2008. A 'signal-free' approach to dendroclimatic standardisation. *Dendrochronologia*, 26: 71–86.
- MELVIN T.M., GRUDD H. & BRIFFA K.R. 2013. Potential bias in 'updating' tree-ring chronologies using Regional Curve Standardisation: Re-processing 1500 years of Torneträsk density and ring-width data. *Holocene*, 23: 364–373.
- MORÉ J.J. 1978. The Levenberg-Marquardt Algorithm: Implementation and theory. *Lecture Notes in Math.*, 630: 105–116.
- NEVALAINEN L. & LUOTO T.P. 2012. Intralake training set of fossil Cladocera for paleohydrological inferences: evidence for multicentennial drought during the Medieval Climate Anomaly. *Ecohydrology*, 5: 834–840.
- NEVALAINEN L., SARMAJA-KORJONEN K. & LUOTO T.P. 2011. Sedimentary Cladocera as indicators of past water-level changes in shallow northern lakes. *Quatern. Res.*, 75: 430–437.
- RINGBOM Å. 2011. The Voice of the Åland Churches: New Light on Medieval Art, Architecture and History. Åland's Museum.
- RINGBOM Å., HAKKARAINEN G., BARTHOLIN T., JUNGNER H. 1996. Åland churches and their scientific dating. Proceedings of the Sixth Nordic Conference on the Application of Scientific Methods in Archaeology, Esbjerg 1993. *Arkæologiske rapporter*, 1: 291–302.
- SEFTIGEN K., BJÖRKLUND J., COOK E.R. & LINDERHOLM H.W. 2015. A tree-ring field reconstruction of Fennoscandian summer hydroclimate variability for the last millennium. *Clim. Dyn.*, 44: 3141–3154.
- SEFTIGEN K., GOOSSE H., KLEIN F. & CHEN D. 2017. Hydroclimate variability in Scandinavia over the last millennium – insights from a climate model-proxy data comparison. *Clim. Past*, 13: 1831–1850.
- SEFTIGEN K., LINDERHOLM H.W., DROBYSHEV I., NIKLASSON M. 2013. Reconstructed drought variability in southeastern Sweden since the 1650s. *Int. J. Climatol.*, 33: 2449–2458.
- SOHAR K., LÄÄNELAID A., ECKSTEIN D., HELAMA S. & JAAGUS J. 2014. Dendroclimatic signals of pedunculate oak (*Quercus robur* L.) in Estonia. *Eur. J. For. Res.*, 133: 535–549.
- TROUET V., ESPER J., GRAHAM N.E., BAKER A., SCOURSE J.D. & FRANK D.C. 2009. Persistent positive North Atlantic Oscillation mode dominated the Medieval Climate Anomaly. *Science*, 324: 78–80.
- TUOMENVIRTA H., DREBS A., FØRLAND E., TVEITO O.E., ALEXANDERSSON H., LAURSEN E.V. & JÓNSSON T. 2001. Nordklima data set 1.0 – description and illustrations. *DNMI Klima*, 08/01: 1–27.
- VÄLIRANTA M., KORHOLA A., SEPPÄ H., TUUTILA E.-S., SARMAJA-KORJONEN K., LAINE J. & ALM J. 2007. High-resolution reconstruction of wetness dynamics in a southern boreal raised bog, Finland, during the late Holocene: a quantitative approach. *Holocene*, 17: 1093–1107.
- WALKER M.J.C. 2005. *Quaternary Dating Methods*. John Wiley & Sons, Chichester, West Sussex, England.
- WILSON R., MILES D., LOADER N.J., MELVIN T., CUNNINGHAM L., COOPER R. & BRIFFA K. 2013. A millennial long March–July precipitation reconstruction for southern-central England. *Clim. Dyn.*, 40: 997–1017.